

This Page Is Inserted by IFW Operations
and is not a part of the Official Record

BEST AVAILABLE IMAGES

Defective images within this document are accurate representations of the original documents submitted by the applicant.

Defects in the images may include (but are not limited to):

- BLACK BORDERS
- TEXT CUT OFF AT TOP, BOTTOM OR SIDES
- FADED TEXT
- ILLEGIBLE TEXT
- SKEWED/SLANTED IMAGES
- COLORED PHOTOS
- BLACK OR VERY BLACK AND WHITE DARK PHOTOS
- GRAY SCALE DOCUMENTS

IMAGES ARE BEST AVAILABLE COPY.

**As rescanning documents *will not* correct images,
please do not report the images to the
Image Problem Mailbox.**



p. 763-769 = (7)

C04B35/111B

J. Am. Ceram. Soc., 79 [3] 763-69 (1996)

Advances in the Grinding Efficiency of Sintered Alumina Abrasives

p d. 03-1996

Andreas Krell* and Paul Blank

Fraunhofer Institut für Keramische Technologien und Sinterwerkstoffe (IKTS), D-01277 Dresden, Germany

Eckhard Wagner and Günter Bartels

Hermes Schleifmittel GmbH & Company, D-22545 Hamburg, Germany

The study relates the grinding power of different grades of sintered alumina abrasives to their microstructures and to basic mechanical properties in comparison with conventionally fused electrocorundum and with an electrofused alumina/zirconia eutectic. Contrary to the traditional approach of the Battelle test, the fracture toughness K_{Ic} of individual grains is measured by a quantitative indentation analysis. Compared with fused corundum, sintered alumina grits exhibit an increased toughness and grinding efficiency, but the further increase of K_{Ic} in the eutectic does not improve the grinding performance. The key parameter for grinding is the inherent hardness of the abrasive. The elimination of flaws by a new approach results in a strong increase in the grinding power of sintered alumina abrasives.

I. Introduction

TRADITIONAL electrofused abrasives consist of quasi-macroscopic grains that represent single crystalline units of about 1/10 to 1 mm size. Obviously, to produce them on a polycrystalline basis to increase by this means the hardness and toughness requires a sufficiently fine-grained microstructure. For about 10 years, microcrystalline alumina grinding materials have been the only sintered ceramics with crystallite sizes less than 1 μm that are produced successfully in amounts of tons per year by an economically profitable sol/gel process. The usual procedure is to prepare a boehmite sol (orthorhombic AlOOH) which is then gelled, dried and sintered. During the first and intermediate stages of sintering, densification and grain growth are associated with simultaneous transformation of transitional alumina phases to corundum ($\alpha\text{-Al}_2\text{O}_3$), whereby it is important that the crystallite size of the transitional aluminas is fairly small (about 50–150 nm). It is now well understood that this transformation and the resulting microstructure depend on the frequency of seeds. At a low frequency of seeds, the transformation starts with a few crystallites, and the fast collective (epitaxial) transformation of a large number of neighboring transitional crystallites generates aggregates of secondary, crystallographically equiaxed $\alpha\text{-Al}_2\text{O}_3$ grains with an internal porosity which is difficult to remove.^{1–4} Seeding can help to avoid this problem, and very different distributions of pores and of crystallite sizes are produced by the different seeding procedures described in a large number of patent applications.^{5–8}

Little is known, however, about the dependence of the technical grinding performance on the microstructure and on basic mechanical parameters. The reason for this discrepancy is that there is an obvious need of an individual mechanical characterization of a statistically sufficient number of abrasive grains,

but most mechanical parameters are determined by methods that are difficult to apply to such small bodies. Common measurements as the Battelle test that assess a large number of unidentified abrasive grains by grinding them in a ball mill (see, for example, U.S. Standard B 74.8-1965, Ball Mill Test for Friability of Abrasive Grains) do not match the advanced level of modern fracture mechanics; they are not useful to derive valid conclusions about the behavior of the grains under the conditions of their technical application.

Further, a high grinding efficiency of an abrasive material cannot be achieved by simply improving its strength and toughness towards increasingly higher values, because a compromise has to be found to meet two contradictory requirements. On the one hand, there is an obvious need of some minimum strength and toughness required for a global stability of the "macroscopic" grinding grain during service. On the other hand, however, wear rounds the working cutting edges that have to be regenerated permanently. For this purpose, strength and toughness on a local scale have to be low enough to allow limited microfracture.

As a consequence of all of these difficulties, most products are developed empirically, and scientific understanding ends with the formation of sol/gel-derived sintered microstructures. Therefore, it is the objective of our work to present first results about a statistical toughness and hardness characterization of aluminous abrasive materials. These basic mechanical parameters of traditional fused and of advanced sintered products are compared with their technical grinding power with the aim of investigating possible approaches for tailoring abrasive grits by an optimization of basic data.

It must be assumed that, under the heavy local load during grinding, the newly formed cutting edge will be stable only if it is distant from flaws (e.g., heterogeneously distributed cracks or regions of increased porosity). As a consequence, the effective hardness at the top of such cutting edges will be the local hardness of more perfect subregions (the "inherent" hardness of the polycrystal), whereas the usual hardness tests give an average hardness when the typical distance of the heterogeneities is less than the size of the indent (in alumina this size is about 20–30 μm with a testing load of 5–10 N and should not be reduced further because of difficulties with the conventional, nonrecording hardness test in the microhardness range⁹). Therefore, possible discrepancies between the average and local hardness have to be considered when relating the hardness to the grinding behavior of sintered abrasive grits with a heterogeneously distributed porosity.

II. Materials and Methods

A survey of the investigated materials is given in Table I. Sintered alumina grits were produced by a sol/gel technology starting with boehmite¹ (purity >99.8% with 0.16% titanium

R. O. Scattergood—contributing editor

Manuscript No. 193540, Received June 1, 1994; approved October 9, 1995.
*Member, American Ceramic Society.

¹Disperal, Condea Chemie, Hamburg, Germany, grain size 5–10 nm, specific surface (BET) 172 m²/g.

Table I. Characterization of Tested Abrasive Materials

Table I. Characterization of Tested Abrasive Materials					
Batch index		Microstructural characteristics	Relative density	Hardness* HV1 (GPa)	Toughness K_{IC} (MPa·m ^{1/2})
FC-B	Fused brown corundum ^a	Single crystalline grains	≈100%	17.4 ± 2.1	2.5 ± 0.8
FC-W	Fused white corundum ^a	Single crystalline grains	≈98%	19.4 ± 0.8	2.2 ± 0.7
FC-R	Fused ruby ^a	Single crystalline grains	≈100%	18.9 ± 1.3	2.8 ± 0.8
FC-Z	Fused eutectic Al ₂ O ₃ /ZrO ₂ ^a	Width of lamellae 0.1–0.5 μm	≈100%	16.3 ± 1.3	4.2 ± 1.4
SG-1	Sintered sol/gel alumina**	Isometric crystallites, coarse size distribution (0.6–6 μm)	85%	14.9 ± 2.8	3.5 ± 1.4
SG-2	Sintered sol/gel alumina	Isometric crystallites (1.1 μm)	86%	(17–20) 14.2 ± 0.9	4.0 ± 0.4
SG-3	Sintered sol/gel alumina	Isometric crystallites, submicrometer size (0.6 μm)	98.2%	(18–21) 20.1 ± 1.3	3.7 ± 0.5
SG-4	Sintered sol/gel alumina**	Platelet-shape crystallites (0.75 μm, thickness 0.11 μm)	95%	(20–25) 18.9 ± 0.7	3.8 ± 0.3
SA-P	Sintered alumina by powder technology	Isometric crystallites (≈1 μm)	99.0%	(19–24) 20.7 ± 0.8	3.8 ± 0.4
				(20–25)	

*For microstructures with flaws (e.g., with a heterogeneous distribution of grain sizes).

*For microstructures with flaws (e.g., with a heterogeneously distributed porosity), the values in brackets give the inherent hardness of subregions that are free of larger defects. These values were estimated from the known crystallite size effect in fine-grained alumina microstructures.¹⁰ ^aDural, supplied by Lonza, Germany. ^bTreibacher Schleifmittel AG, Villach, Austria. ^cH. C. Starck GmbH & Co. KG, Lauffenburg, Germany. ^dNZ-Alundum E847, Saint-Gobin/Norton, Northboro, MA. ^eSapphire Blue, Hermes Schleifmittel GmbH & Co., Hamburg, Germany. ^fCubitron, Minnesota Mining and Manufacturing Comp., Saint Paul, MN.

and 0.02% silicon as the main impurity components). For SG-1 and SG-2, the sol was prepared at pH 3 (adjusted by HNO₃) with 0.5% magnesia and 4% transitional alumina seeds (>90% γ-Al₂O₃) to promote the transformation on sintering as described previously;⁸ a blue color is generated by cobalt doping. Corundum (α-Al₂O₃) seeds were used for SG-3. All given concentrations relate to the final amount of alumina obtained from the boehmite. Gelation occurred after adding magnesia as solution of a salt. The gel was dried, broken, calcined and sintered between 1390° and 1450°C for 10 min to give abrasive grains with microstructures as described by Figs. 1(a–c) and by the data in Table I. Note the relatively high residual porosity (Figs. 1(a) and (b)) and the wide crystallite size distribution (Fig. 1(a)) in some of the microstructures. In SG-1, both the microstructural crystallite size and the pore distributions exhibited a significant scatter when different grinding grains were compared.

As a result of the impossibility of dispersing seeds in the sol on the nanometer level of the boehmite, all sol/gel-derived microstructures contain typical flaws. Figure 2 gives an example for the batch SG-3 obtained with α-Al₂O₃ seeds. Careful seeding minimizes both the frequency and the size of such flaws but cannot avoid them absolutely. It is obvious that even small defects which are hardly seen on polished surfaces will reduce the measured hardness.

Homogeneous samples with isometric crystallites and with a very low residual porosity have been prepared by pressureless sintering using very pure alumina (SA-P in Table I).¹¹ The type of microstructures follows that shown in Fig. 1(c) but without flaws as shown in Fig. 2 for sol/gel products. Like the dried gel, these materials had been broken before sintering to get a grit with sharp edges.

To test the possible chances for future investigations, supplementary comparative hardness and toughness measurements were performed with three materials that had not been included in the present grinding investigations but which might represent interesting alternatives: two purer fused grades (FC-W, FC-R in Table I) and another commercial sintered alumina abrasive (SG-4 in Table I). The platelet-shaped microstructure of the latter is described by Fig. 1(d).

For hardness and toughness measurements, the abrasive grains with an average size of about 0.6 mm were mounted in epoxy resin, ground, and polished. The Vickers hardness was measured with a load of 10 N; lower loads are avoided because they result in questionable hardness values,⁹ whereas at higher testing loads the polished grains are pressed into the mounting epoxy resin. Since sintered alumina microstructures occasionally happen to exhibit inelastic relaxation for more than 10 s,¹² the maximum load was applied for 30 s. The typical standard deviation on measuring polished polycrystalline specimens is

±0.30...0.60 GPa for macroscopic bodies; it was larger here, due to microstructural inhomogeneities.

The indentation fracture toughness was derived from radial crack lengths, using an approach proposed by Anstis *et al.*¹³ Their formula contains a constant $\xi = 0.016$ from an adjustment of their procedure to other K_{IC} results for a wide range of ceramics. As suggested by the results of Guillou *et al.*,¹⁴ this constant parameter is probably not as material-independent as originally supposed. Therefore, $\xi = 0.023$ was used here, which results from a fit of Anstis's relationship to the alumina data presented there. Only one indentation was placed into the center of the examined "macroscopic" grinding grains, and only indents with a regular system of four radial cracks were analyzed. The analyzed grinding grains were large compared with the crack length (maximum crack length $2c \approx 250 \mu\text{m}$ at minimum $K_{IC} \approx 0.9 \text{ MPa}\cdot\text{m}^{1/2}$).

The distribution of fracture toughness resulting from the observed crack lengths was assessed in accordance with usual Weibull statistics by ranking all measured data and calculating the probability of the i th of N values with the estimator $(i - 0.5)/N$.¹⁵ Conventionally, Weibull statistics are used to describe inherent flaw distributions in strength tests or to analyze the resulting strength distribution itself. Of course, Weibull statistics can also be regarded as a pure mathematical instrument that is applicable beyond this special background, but the actual reason to use this procedure here was that most abrasive products contain many flaws with a size of a few micrometers which affect the indentation crack length and, in this way, the calculated (local) toughness. Such flaws are, for example, pores or porous subregions typical for most of the sol/gel-derived alumina products (Fig. 2). Additionally, cracklike flaws are introduced when the fused or gelled and dried compact materials are broken down. In the experience of the authors, the characterization of abrasive materials by the distribution of indentation toughness data usually gives straight Weibull plots. It is suggested that these microflaw-dependent K_{IC} are close to a strength characterization of the products and should only cautiously be compared with the known toughness data of compact ceramics.

The grinding performance was tested by abrading the plane cross section of a slotted steel tube with flexible disks where the abrasive grits are fixed by a special resin. The welded tube was produced from scale-free cold-rolled sheet steel (German standard St W 22 (DIN 1543)), and had a diameter of 180 mm and a wall thickness of 1 mm. The abrasive disk and the steel tube rotated with speeds of 6000 and 16.3 min⁻¹, respectively. The clamping angle of the flexible disk was 24°; the contact force was kept constant at 30 N by dead-weight loading for the whole experiment. The measured quantity was the removed mass of steel for given grinding durations.

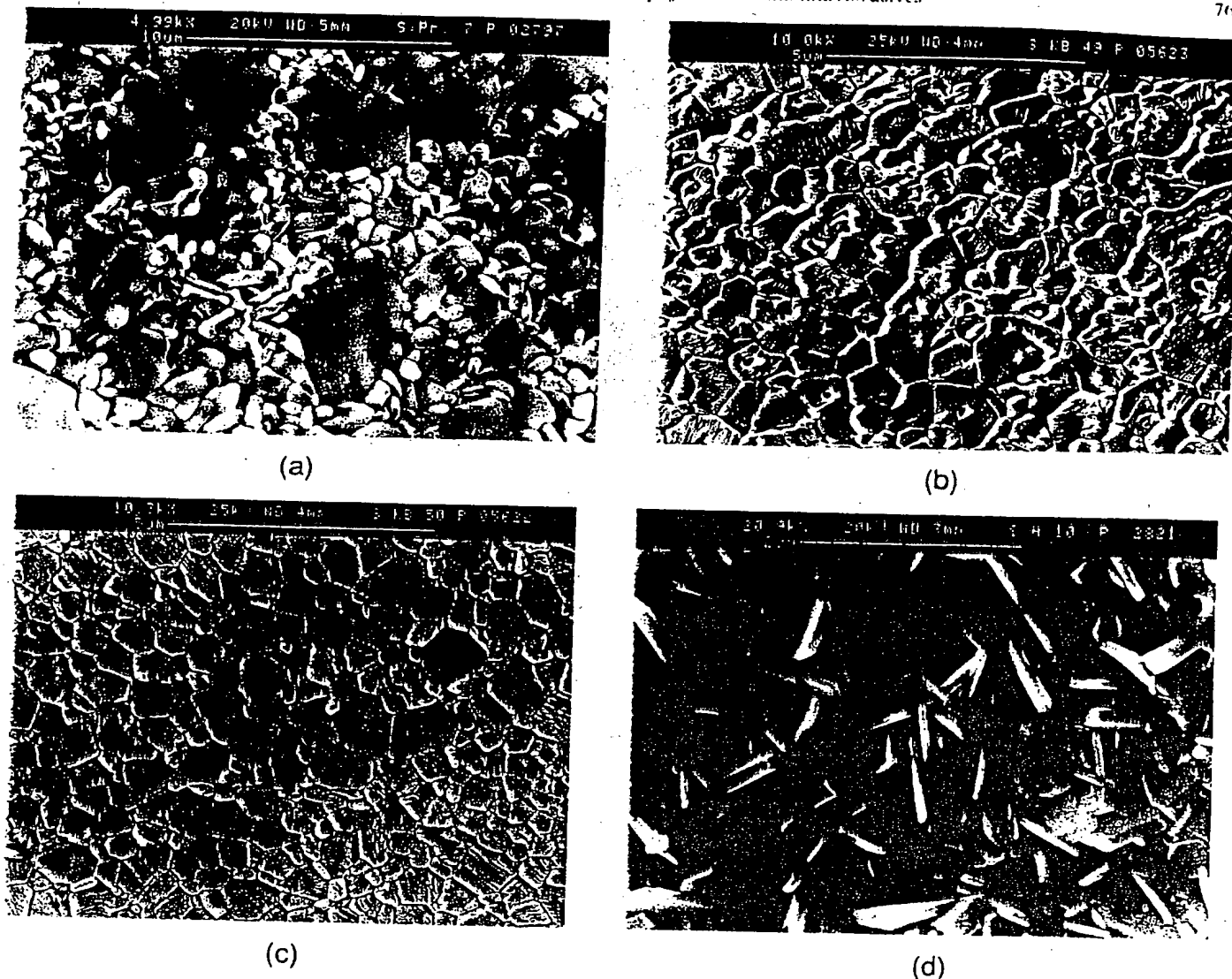


Fig. 1. Microstructure of sintered alumina abrasive grits produced by sol/gel approaches. Thermally etched surfaces. Data are given in Table I. (a) Sapphire Blue (SG-1). (b) fine-grained porous microstructure (SG-2). (c) submicrometer dense material (SG-3). (d) Cubitron (SG-4).

The appearance of the flexible disks after the tests was similar for all materials; i.e., different grinding was never associated with different pullout frequencies of grains from the binder of the disks. Hence, differences in the plots are caused by differences in the behavior of the ceramic grits themselves.

III. Results

The average hardness and toughness results are listed in Table I. The average toughness values of most of the sintered aluminas (SG-2 through SG-4, SA-P) are considered as similar within the limits of confidence. The slightly higher and lower averages as well as the wide distributions of the $\text{Al}_2\text{O}_3/\text{ZrO}_2$ eutectic and of SG-1, respectively, turned out to be reproducible characteristics of the microstructures. The same is true for the differences in the hardness in spite of the sometimes large standard deviations.

Weibull plots of the toughness distributions are given in Fig. 3(a) for fused abrasives. The toughness of electrofused corundum does not present any surprises. For brown corundum, both the average toughness and its standard deviation agree with the known K_{IC} anisotropy of sapphire.^{16,17} The broader width of distribution in fused $\text{Al}_2\text{O}_3/\text{ZrO}_2$ is probably related to the typical eutectic microstructure. On the contrary, similar

results are observed for brown corundum, white corundum, and ruby.

In addition to Table I, Fig. 3(b) gives the toughness distributions measured for the sintered sol/gel-derived materials. In batch SG-1 there is an obvious correlation of the broad distributions of the fracture toughness and of grain sizes (Fig. 1(a)), a result that is not surprising, with the known effect of crystallite sizes on the toughness of sintered alumina.¹⁸ All other samples in Fig. 3(b) show remarkably similar results. Note the surprisingly small influence of the porosity and of the crystallite size in the range between about 0.5 and 1 μm .

In Fig. 3(c), the abrasive grit produced by a powder approach exhibits the same toughness distribution as the sol/gel-derived materials of comparable microstructures. The average toughness of all of the sintered alumina microstructures is close to the typical level of polycrystalline alumina (about 3.5–4.0 $\text{MPa}\cdot\text{m}^{1/2}$).

The results of the grinding experiments are shown in Fig. 4, where the even character of the curves indicates a very small scatter of the individual data. The differences between the curves in Fig. 4 were confirmed by repeated tests.

In Fig. 4(a), the grinding efficiency of the alumina/zirconia is seen to exceed that of the brown fused corundum. At a similar hardness, this behavior has to be attributed to the higher toughness of the eutectic, which is an indication of the increased

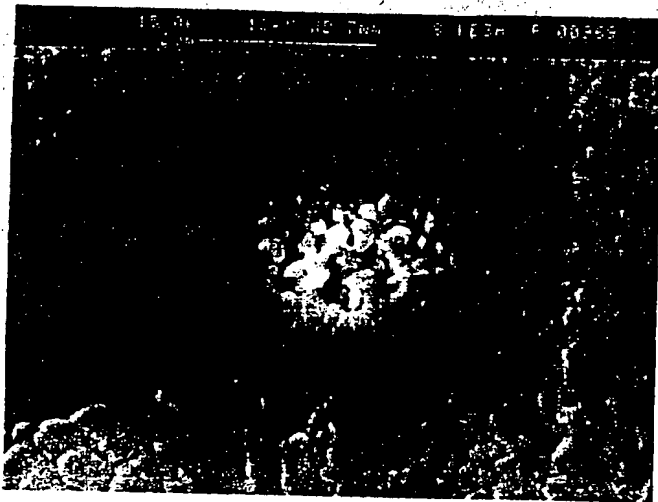
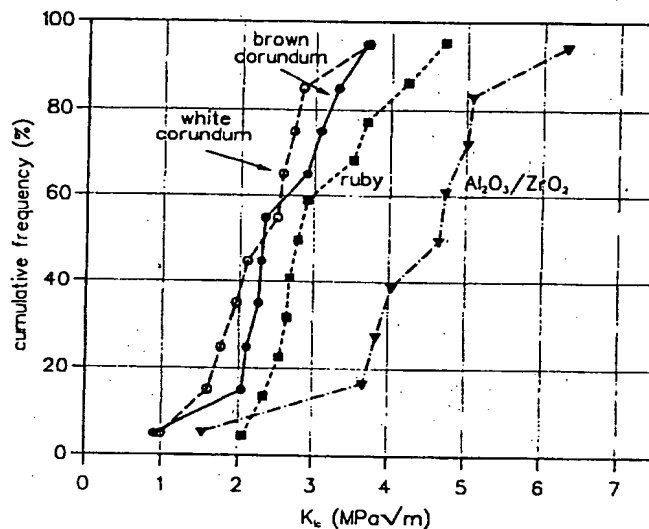


Fig. 2. Small porous defect in sintered sol/gel alumina (α -seeding).

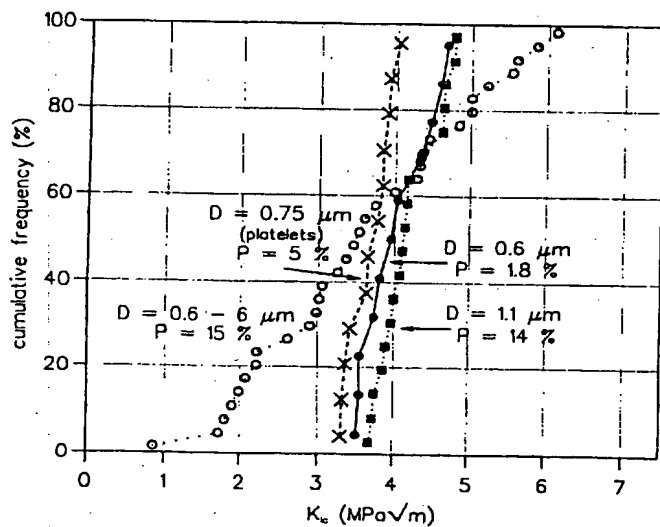
mechanical stability of the abrasive grains. Surprisingly, however, the sintered material SG-1 shows an even better performance in spite of its high residual porosity (and, consequently, low hardness) and its toughness, which is only intermediate between the fused eutectic and the brown corundum.

An explanation might be some difference between the *measured* hardness, which gives an average value for the whole microstructure, and the *effective, local* hardness of the porous, heterogeneous sintered microstructure, as suggested in the introduction. If this explanation is right, the existence or the elimination of this large porosity should not affect the grinding behavior. The tests presented in Fig. 4(b) were performed to test this idea. All sol/gel-derived grits showed the same grinding power independent of large differences in their porosities and crystallite size distributions.

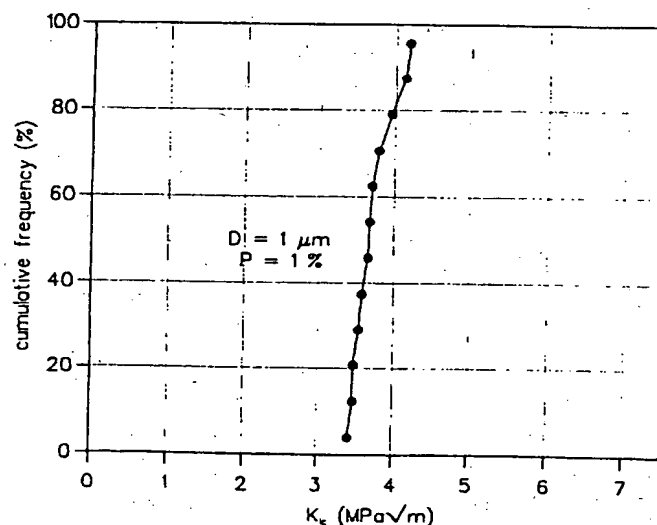
A surprisingly strong effect of different alumina processing is shown in Fig. 4(c). Replacing sol/gel approaches by a powder process results in an advanced abrasive that exhibits an improvement similar to that achieved using sol/gel abrasives compared to electrofused grits. In additional tests, the grinding result of the powder approach in Fig. 4(c) was exactly reproduced with other sintered abrasives (average crystallite sizes 0.5–1 μm) produced by *different* shaping approaches like cold



(a)

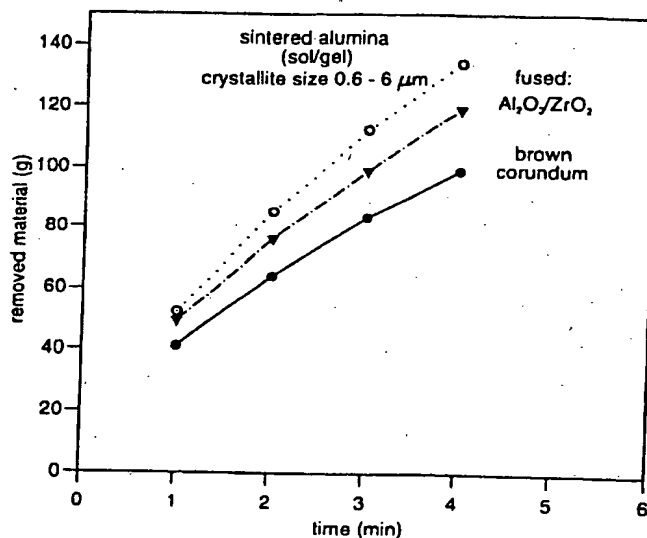


(b)

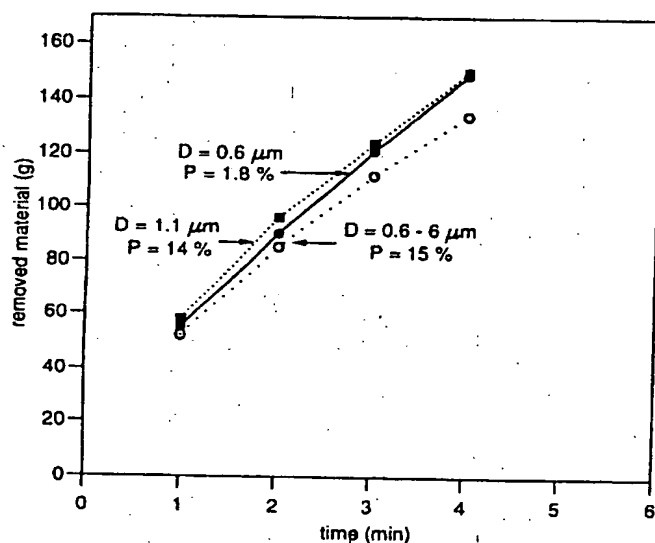


(c)

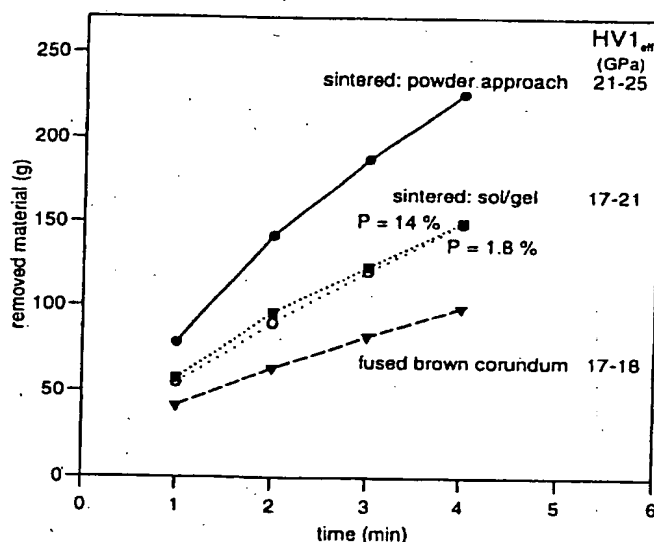
Fig. 3. Fracture toughness distributions. D—average crystallite size, P—porosity. (a) Fused abrasives, (b) sintered sol/gel-derived abrasives, (c) sintered alumina prepared by a powder approach (SA-P).



(a)



(b)



(c)

Fig. 4. Grinding performance of different fused and sintered grits on the basis of alumina. (a) Electrofused grades and coarsest sintered (sol/gel-derived) material SG-1, (b) sol/gel-derived sintered abrasives SG-1 through SG-3, (c) alumina abrasives produced by electrofusion, sol/gel approaches, and powder technology.

isostatic pressing or pressure filtration. This observation substantiates the presentation in Fig. 4(c), which does not display a random selection of different samples but distinguishes electrofusion, sol/gel processing, and the powder approach as groups of alumina abrasives with a generally different grinding efficiency.

III. Discussion

In the fused materials, the measured hardness of the brown corundum grit is lower than the typical data for pure sapphire ($HV1 \approx 19$ GPa)—an obvious consequence of impurities in this technical product. In the eutectic, it is the zirconia phase which decreases the hardness but improves the fracture toughness because of the lamellar microstructure and, probably, some stress-induced martensitic transformation of metastable ZrO_2 .¹⁹ The improvement in toughness is quite remarkable compared with the "crystallographically averaged" toughness of sapphire of about $2.5 \text{ MPa}\cdot\text{m}^{1/2}$ which can be estimated from published

data.^{16,17} The very low fracture toughness of brown fused corundum means a low resistance of the cutting grain edges to fracture and explains the low grinding efficiency compared with the fused eutectic.

With the results in Figs. 4(a) and (b), it appears that under the applied grinding conditions the toughness of any of the sintered aluminas is sufficient to supply a high global stability of the grains as an essential for a high grinding power: Independent of their hardness, all materials with an average toughness $>3 \text{ MPa}\cdot\text{m}^{1/2}$ exhibit a much better grinding power than fused brown corundum. The comparison of Fig. 3(b) with Fig. 4(b) confirms that only the average toughness is important, without an effect from the width of the distribution: reducing the width of grain size and toughness distributions at a similar porosity (SG-1 \rightarrow SG-2) remains without consequences to the grinding behavior.

This interpretation does not explain, however, the superior grinding behavior of the sintered porous alumina SG-1 compared with the Al_2O_3/ZrO_2 eutectic (Fig. 4(a)), which exhibits a

higher hardness and toughness. Several possible reasons have to be taken into account. Let us first discuss the effect of the toughness.

The grinding advantage of the sintered alumina abrasives compared with the eutectic, which is characterized by an even greater global stability of the grinding grains (exemplified by the high average K_{IC}), substantiates the idea of an altered role of the toughness (or strength) beyond some required minimum, as presented in the introduction. A high strength on a microscale hinders the regeneration of sharp cutting edges, and in plots like Fig. 4 this results in curves with slopes that decrease with time. In Fig. 4(a) this effect is more pronounced in the behavior of the (very tough) fused eutectic than in the sintered alumina. If abrasive grains are very strong also on their macroscale, another consequence may be an increased pullout and loss of grains from the tool, again associated with a drop of the grinding efficiency. The results plotted in Fig. 4 suggest that it is just the moderate toughness of the sintered alumina abrasive that gives rise to its superior grinding performance.

Another important item is the influence of the residual porosity in the sintered alumina abrasive SG-1 (Fig. 1(a)) on fracture and hardness. Under the extreme conditions near cutting edges, the pores will act as stress concentrators and initiate microfracture which regenerates sharp cutting edges, a feature that needs to be investigated in future microscopic investigations. It was suggested that, if microfracture is initiated by pores, the just-generated microscopic cutting edge which now, obviously, withstands the cutting forces for a while is characterized by denser regions with a locally increased hardness related to the crystallite size. Dense alumina ceramics with crystallite sizes as shown in Fig. 1(a) (about 0.6–6 μm) have a hardness between 17 and 20 GPa when measured with loads of 10–100 N.¹⁰ This local hardness of the sintered alumina microstructure significantly exceeds that of the fused eutectic, which will always (on any scale) be influenced by the existence of the less hard zirconia lamellae neighboring the alumina phase.

Of course, with Fig. 4(a) only, this idea would be no more than a hypothesis which is difficult to substantiate theoretically, because nothing is known about the critical distance an active cutting edge will have from the closest flaws. However, Fig. 4(b) gives clear evidence that the high porosity in SG1 and SG-2 (which is the obvious cause of the very low hardness) has no influence on the advantageous behavior of the sol/gel abrasives compared with the fused eutectic: the elimination of porosity (SG-2 \rightarrow SG-3) has only a minor influence on the grinding behavior. Therefore, it must be a porosity-independent, inherent hardness which is a key parameter (beyond some required minimum toughness).

At this point, however, a more straightforward question appears: if the range of very small crystallite sizes used for the tests in Fig. 4(b) is really associated with a strong increase of the hardness,¹⁰ what is then the reason for the lack of any crystallite size effect in the grinding results of Fig. 4(b)? To answer this question requires a closer look onto the flaw populations in the investigated microstructures. It has to be emphasized that in Table I the upper limit of the suggested inherent hardness level refers to microstructures with a very low frequency of flaws. Small defects as shown in Fig. 2 are not completely eliminated in a sol/gel process, and they are assumed to be stable anywhere in the cutting abrasive grain, even close to an active cutting edge. Assuming that such flaws deteriorate the effective hardness and the grinding power, the conclusion was to return to "traditional" powder processing but, of course, important improvements had to be realized to associate the advantage of advanced corundum powders (small crystallite sizes giving a high density at low temperatures and little grain growth) with an extremely low frequency of flaws in the green (not yet sintered) body.¹¹ This highly perfect microstructure of the formed bodies before sintering is essential for homogeneous densification to get a product with few and small residual flaws. The final result of this development is a microstructure like sample SA-P which comes close to the upper limit of the

expected inherent hardness and exhibits a dramatic improvement of their grinding power compared with the sol/gel-derived abrasives. The observation that a very high grinding efficiency was reproduced within the framework of powder processing by different shaping approaches further substantiates the idea that the key to this progress is the elimination of the typical flaws associated with sol/gel technologies (Fig. 2). Investigations with submicrometer crystallite sizes giving a hardness of HV1 = 25–30 GPa in pressureless sintered pure alumina grits are under way to exhaust further the potential advantages of this approach.

With a similarly low toughness of the three fused Al_2O_3 abrasives in Fig. 3(a), no significant improvement of the grinding behavior can be expected when replacing one grade of electrofused alumina by another. Also, the surprisingly similar toughness of sol/gel-derived submicrometer grinding grains with very different microstructures (SG-3 and SG-4 in Figs. 1(c–d)) as given by Fig. 3(b) at a similar hardness excludes a strong effect of the crystallite morphology.

IV. Conclusions

Individual characterization of microstructure and mechanical properties of abrasive grains is possible and enables a better understanding of the technical performance. The statistical assessment of the indentation toughness gives a valuable characterization of the mechanical stability of individual grinding grains and provides a quantitative measure for the distribution of this property, even if the effect of the average toughness on the grinding power of the abrasives turns out to be much more important than the width of the distribution.

Because of its very low fracture toughness, brown fused corundum exhibits a lower grinding efficiency than fused $\text{Al}_2\text{O}_3/\text{ZrO}_2$ eutectics or sintered alumina.

A certain minimum level of the fracture toughness is required to achieve a global stability of the grains under the extreme (dynamic) mechanical conditions in grinding. The high grinding efficiency achieved with all sintered alumina abrasives compared with electrofused corundum indicates that this lower limit of the required toughness is in the range of about $3 \pm 0.5 \text{ MPa}\cdot\text{m}^{1/2}$. A further increase of the toughness above of about $4 \text{ MPa}\cdot\text{m}^{1/2}$ did not provide additional advantages here. The identification of active wear mechanisms will require extended microscopic work, but already the present investigations indicate that an exceptionally high grinding efficiency can be expected with a toughness in the range between about 3.5 and $4 \text{ MPa}\cdot\text{m}^{1/2}$ (whereby it has to be emphasized that the optimum range for the toughness depends on the applied grinding conditions and on the characteristics of the ground material).

Given some required minimum toughness, the key parameter in grinding appears to be the local, inherent hardness close to the active cutting edges. This inherent hardness increases with reduced crystallite size, but to exhaust the potential hardness and grinding power additionally requires a microstructure with few flaws. Powder processing is a promising way to produce such abrasives. First results show an increase in the grinding efficiency compared with sol/gel-derived alumina, a progress that compares with the former step from fused to sol/gel corundum.

References

1. F. W. Dynys and J. W. Halloran, "Alpha Alumina Formation in Alum-Derived Gamma Alumina," *J. Am. Ceram. Soc.*, **65** [9] 442–48 (1982).
2. A. Krell and G. Sickert, "Influence of $\gamma\text{-Al}_2\text{O}_3$ Concentrations in Raw Alumina Powders on Their Processing and Sintering Performance and on the Resulting Mechanical Properties" (in Ger.), *Silikatechnik*, **35** [7] 204–207 (1984).
3. G. L. Messing, M. Kumagai, R. A. Shelleman, and J. L. McArdle, "Seeded Transformations for Microstructural Control in Ceramics," pp. 259–71 in *Science of Ceramic Chemical Processing*. Edited by L. L. Hench and D. R. Ulrich. Wiley, New York, 1986.
4. G. L. Messing and J. C. Huling, "Transformation, Microstructure Development and Sintering in Nucleated Alumina Gels," pp. 669–79 in *Third Euro-Ceramics*, Vol. 1. Faenza Editrice Iberica, San Vicente, Spain, 1993.

- "R. Bauer, "Process for Producing Alumina Bodies," Eur. Pat. Appl. EP-168606, January 22, 1986.
- "H. G. Sowman and M. A. Leitheiser, "Non Fused Aluminium Oxide-Based Abrasive Material, a Process for its Production and Abrasive Products Comprising the Said Abrasive Mineral," Eur. Pat. Appl. EP-24088, January 25, 1984.
- "M. Kumagai and G. L. Messing, "Ceramic Sintered Body," Eur. Pat. Appl. EP-172764, February 26, 1986.
- "G. Bartels, G. Becker, and E. Wagner, "Process for the Production of a Ceramic Polycrystalline Abrasive," U.S. Pat. No. 5034360, July 23, 1991 (German priority DE-3525175, July 15th 1985).
- "A. Krell, "Load Dependence of Hardness in Sintered Submicrometer Al_2O_3 and ZrO_2 ," *J. Am. Ceram. Soc.*, 78 [5] 1417-19 (1995).
- "A. Krell, "Grain Size Dependence of Hardness in Dense Submicrometer Alumina," *J. Am. Ceram. Soc.*, 78 [4] 1118-20 (1995).
- "A. Krell and P. Blank, "Sintered Alumina—Hard and Strong Like Hot-Pressed $\text{Al}_2\text{O}_3/\text{TiC}$ Composites," pp. 507-11 in Ceramic Transactions, Vol. 51, *Ceramic Processing Science and Technology*, Edited by H. Hausner, G. L. Messing, and S.-I. Hirano. American Ceramic Society, Westerville, OH, 1995.
- "A. Krell, "Vickers Hardness and Microfracture of Single and Polycrystalline Al_2O_3 ," *Krist. Tech. (Crystal Science and Technology)*, 15 [12] 1667-74 (1980).
- "G. R. Anstis, P. Chantikul, B. R. Lawn, and D. B. Marshall, "A Critical Evaluation of Indentation Techniques for Measuring Fracture Toughness: I. Direct Crack Measurements," *J. Am. Ceram. Soc.*, 64 [9] 533-38 (1981).
- "M.-O. Guillou, J. L. Henshall, R. M. Hooper, and G. M. Carter, "Indentation Fracture Testing and Analysis, and Its Application to Zirconia, Silicon Carbide and Silicon Nitride Ceramics," *J. Hard Mater.*, 3 [3/4] 421-34 (1992).
- "J. D. Sullivan and P. H. Lauzon, "Experimental Probability Estimators for Weibull Plots," *J. Mater. Sci. Lett.*, 5 [12] 1245-47 (1986).
- "S. M. Wiederhorn, "Fracture of Sapphire," *J. Am. Ceram. Soc.*, 52 [9] 485-91 (1969).
- "P. F. Becher, "Fracture-Strength Anisotropy of Sapphire," *J. Am. Ceram. Soc.*, 59 [1/2] 59-61 (1976).
- "B. Mussler, M. V. Swain, and N. Claussen, "Dependence of Fracture Toughness of Alumina on Grain Size and Test Technique," *J. Am. Ceram. Soc.*, 65 [11] 566-72 (1982).
- "M. Rühle and A. H. Heuer, "The Martensitic Reaction in $t\text{-ZrO}_2$," pp. 14-32 in *Advances in Ceramics, Vol. 12, Science and Technology of Zirconia II*, Edited by N. Claussen, M. Rühle, and A. H. Heuer. American Ceramic Society, Columbus, OH, 1984. □

THIS PAGE BLANK (USPTO)